Malaria Detection Using Local Composition Pattern

Malaria Detection Using Local Composition Pattern

J A Ovi[1], M E Haque[2], A Kalam[3], S A Jarin[4], M S Ali[5], M Hasan[6]

[1,2,3,5,6]Dept. of Computer Science and Engineering, East West University, Bangladesh
[4]Dept. of Genetic Engineering and Biotechnology, East West University, Bangladesh

E-mail: *jesan@ewubd.edu*[1], *enamulhaque028@gmail.com*[2], *abukalam973@gmail.com*[3], *sa.zarrin041@gmail.com*[4], *alim@ewubd.edu*[5], *munna09bd@gmail.com*[6]

Abstract. Malaria is a major global health problem. Every year thousands of people have been died because of this harmful disease. It is a life-threatening disease that is triggered by the "night-biting" mosquitoes known as the Anopheles mosquitoes. They normally bite at day time. In this paper, to detect malaria parasite in the bloodstream, an image processing algorithm has been developed. Our proposed approach can classify malaria-infected images from patient's blood samples by extracting red blood cells (RBCs) from the images. Malaria detection using Local Composite Pattern (LBP) outperforms in comparison with the existing traditional approaches.

1. Introduction

Malaria is a disease that is infectious and a significant global health issue. According to the World Health Organization (WHO), 200 to 300 million infections occur every year for this diseases [1] [2]. The risk of malaria is high specially in developing countries. As it affects millions of people, it is a loss of productivity and hampers economical condition which has been estimated at US$800 million in 1995[3]. in order to control malaria, efficient detection mechanism need to be introduced. To detect this, We need a procedure by which we can accurately and rapidly identify malaria which facilitates prompt treatment.

There are a lot of methods such as rapid antigen, Polymerase Chain Reaction (PCR), fluorescent microscopy detection methods- based methods and so on by which malaria can be detected but the most commonly and widely used technique is known as microscopic diagnosis or light microscopy which is very sensitized and highly certain [4][5][6][7]. Under the microscope, the microscopic experiment involve remarkable and head-on envision of the parasite. From the clinical laboratory to the field surveys, the straight microscopic envision of the parasitoid on the deep or thin blood stain has been the approved technique for the malaria identification. It is the most proficient and veracious diagnostic technique. There are a lot of advantages of this microscopy. It is feasible to quantify and distinguish between species and parasitaemia of the parasites. The marginal costs[8] of tests are very low. The goal of this literature is to enhance microscopy by abolishing its most significant limitation: relying for diagnostic accuracy on the execution of a human operative[9]. They present parasite segmentation techniques in tint pictures. The plan of action is based on HSV color space segregation of parasites and RBCs which uses image variability[10]. They juxtapose three distinguish identification categorization schemes and draw a conclusion to the identification, life cycle and species spotting piece of work can be successfully carried out through a single multi - class grouping[11].

There are some disadvantages of this technique. The cost of the microscopy is extremely high. There are also some additional cost such as to training and maintain the microscopy which is very time consuming.

The goal of this experiment is to improve microscopy by eliminating it's limitation. This is gained by establishing computer vision or a digital image processing algorithm[12][13][14]. There are some image processing algorithms such as Local Composition Pattern (LCP), Local Derivative Pattern (LDP), Local Binary Pattern (LBP) and so on[15][16][17][18][19][20]. With the help of the algorithm, a reliable system can be established to automate the examination of blood steams. This technique can be used in segmenting uninfected and infected red blood cells.

2. Literature Review

This paper comes up with an robust screening method that can detect malarial parasites. Though there are some existing diagnostic methods that are dependent on skilled operators. Proper training is also required for these methods. Compared to other techniques, our proposed algorithm gives better result. If this algorithm is applied in a convenient application, it can detect cells that are contaminated and uninfected. Two sets of data have been used. Infected and uninfected cell images are two classes containing a total of 27,558 images.

The aim of this study was to established a method for detecting malaria parasites that shows significant improvement over other techniques [21] [22] and has been widely carried out.

3. LOCAL PATTERNS

3.1. Local Binary Pattern (LBP)

T. Ahonen [20] et al introduced local binary pattern. A block of 3×3 is taken from given image and each component is labeled using a threshold derived from the difference between neighboring pixel and central pixel and converted into a binary number shown in figure 1.

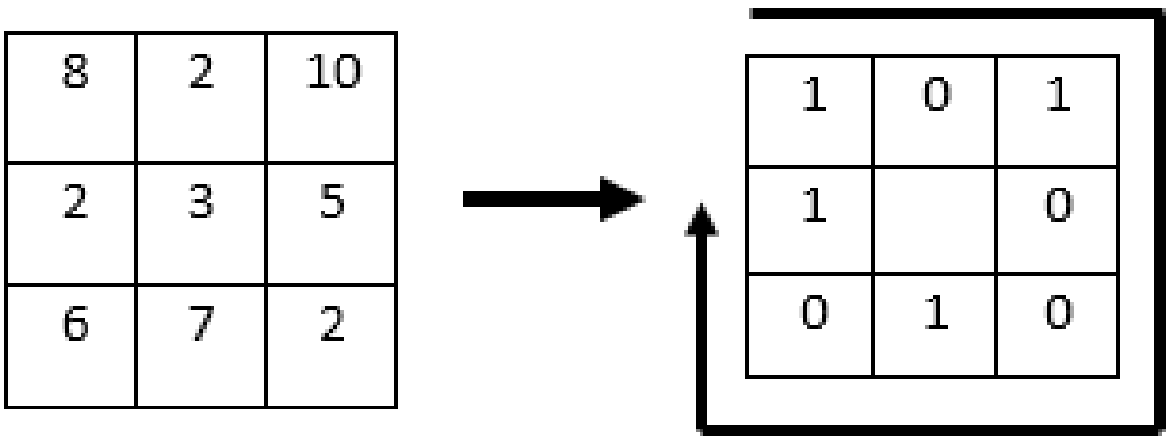

Figure 1. Micro pattern of LBP for 3×3 block.

3.2. Local Derivative Pattern (LDP)

LDP is a descriptor for image features that calculates the extreme radial values to encode the texture of an image [23]. This descriptor uses the Kirsch mask to calculate the border response in eight directions. It is a more robust image descriptor function and much more accurate and standardized than LBP.

3.3. Local Composition Pattern (LCP)
Each part is labeled in LCP by taking center pixel and neighboring pixel derivatives as comparable to LBP depicted in figure 2.

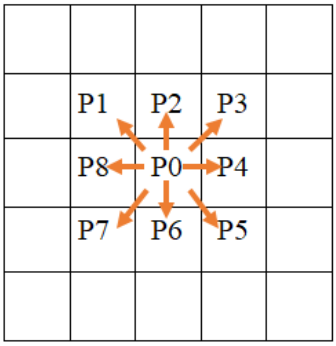

Figure 2. First order derivative along radial direction

Two other derivation is made along the vertical and horizontal direction shown in fig. 3. An edge detection mask is then placed on as an LDP mask as shown in fig. 4. Then we apply the equation (5) where the labeling is verified for neighbors with a modified value. We use a threshold evaluated by summing the values we receive from the addition of derivatives from the vertical and horizontal direction.

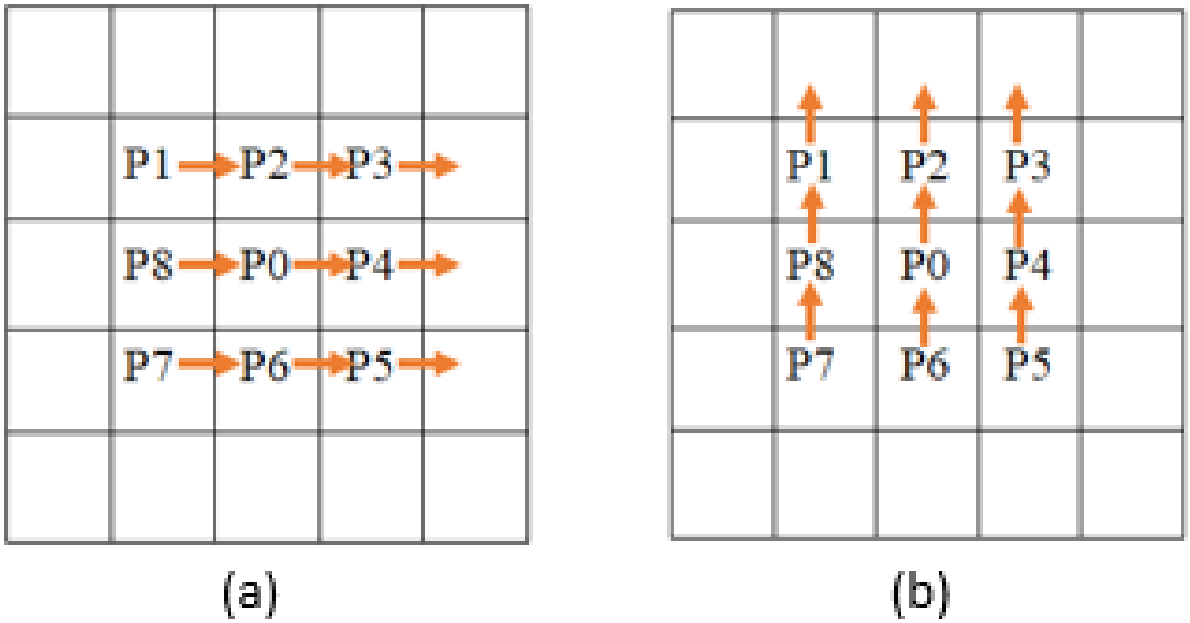

Figure 3. (a) Horizontal direction first order derivative (b) Vertical direction first order derivative

4. LOCAL COMPOSITION PATTERN
In this process the provided image is divided into 6×6 domains. it is delineated in figure 1.

$$\begin{bmatrix} -1 & 0 & 3 \\ -3 & 0 & 5 \\ -3 & 0 & 1 \end{bmatrix} \begin{bmatrix} -1 & 0 & -3 \\ -2 & 0 & 3 \\ -2 & 0 & -2 \end{bmatrix} \begin{bmatrix} 3 & 0 & -1 \\ 5 & 0 & -2 \\ -3 & 0 & 1 \end{bmatrix} \begin{bmatrix} 1 & 0 & -1 \\ 3 & 0 & -1 \\ -3 & 0 & -2 \end{bmatrix}$$

(M_1) (M_2) (M_3) (M_4)

$$\begin{bmatrix} 5 & 0 & 3 \\ 3 & 0 & -2 \\ 5 & 0 & -1 \end{bmatrix} \begin{bmatrix} 1 & 0 & -1 \\ -1 & 0 & -2 \\ -1 & 0 & -1 \end{bmatrix} \begin{bmatrix} -3 & 0 & 5 \\ -2 & 0 & 2 \\ -1 & 0 & -2 \end{bmatrix} \begin{bmatrix} -1 & 0 & 1 \\ 5 & 0 & -2 \\ 1 & 0 & -2 \end{bmatrix}$$

(M_5) (M_6) (M_7) (M_8)

Figure 4. Edge detection mask.

Let $P0$ as the central component in domain I(P) and pi components as the radial direction neighbor, where I = 1,2,3, ... 8. The summation of first order derivatives along the radial directions is TDr and is shown in figure 2. It is characterized as equation (1).

$$TD_r = \sum_{i=1}^{8} (I_{p_0} - I_{p_i}) \tag{1}$$

The sum of the first-order imitative TZd along the direction of 0^0 and the addition of the first-order imitative TNd along the direction of 90^0 are then interpreted as equation (2) and equation (3) respectively. This is shown in figure 3.

$$TZ_d = \sum_{i=1}^{8} (I_{p_i} - I_{p_m}) \tag{2}$$

$$TN_d = \sum_{i=1}^{8} (I_{z_i} - I_{p_n}) \tag{3}$$

It uses 8 different directional masks with different values. Let Mj be the mask, where the eight directions are j = 1,2,3,...,8. Figure 5 indicates the mask.

We use this mask in various neighboring pixels, which is shown in figure 6 and shown as equation (4).

$$I'(Z_i) = I(Z_i) \times M_i \tag{4}$$

The neighboring points new value can be found by using equation (5). The directional response for each neighboring pixels in horizontal and vertical direction have been checked. When both directions are less than or greater than 0 then the directional derivatives of the component is summarized with the components edge response value and the outcome is further divided by 2. Again, if the horizontal directional response is lower than zero and the vertical direction is lower than zero, or vice versa, the directional response, which is higher than zero, is taken and the edge response is applied to it and divided by 2.

By the smmmation of the derivative of first order along 90^0 direction and the sum derivative of first order along 0^0 direction the threshold function 'T' has been calculated. For each LCP

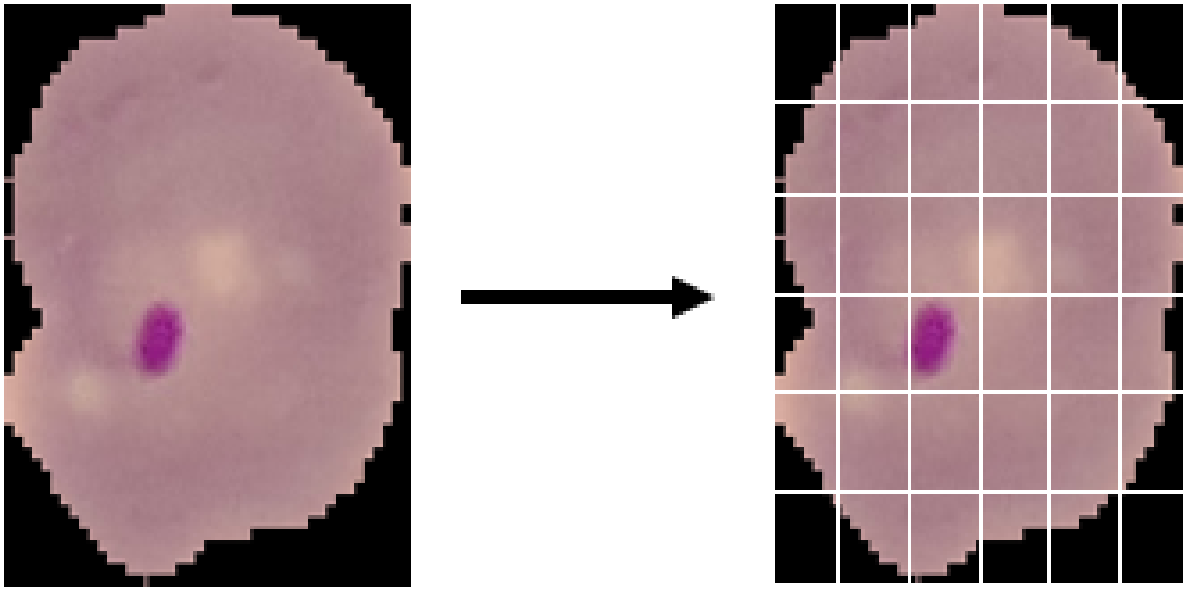

Figure 5. Image divided into 6x6 region

103	50	20
65	30	45
85	55	25

(a)

515	0	60
195	X	-90
425	0	-25

(b)

Figure 6. (a) Applied mask in a 3×3 block of Original image (b) Applied mask in a 3×3 block of Eight direction edge response

pattern, different threshold values are found that can extract more important features and distinguish them from the image given.

To obtain the local composition pattern, we use the equation (1) to calculate the total value of the first order derivatives TDr along the radial directions and the equation (2) and (3) to obtain the total value of the directional derivative along the direction of 0^0 and 90^0. The (4) equation is then used. Equation (5) is used to measure the new adjacent pixel value. To extract important local features from the image, a threshold from equation (7) and a separate threshold value from equation (8) are then applied. The extracted LBP, LDP and LCP image features are represented in Figure 7.

$$f_i(x) = \begin{cases} \frac{I'_{0^0}(P_i)+I'_{90^0}(P_i)+I'(P_i)}{2}, \; if \; \mathrm{I'}_{0^0}(P_i) \geq 0 \\ and \\ \mathrm{I'}_{90^0}(P_i) \geq 0 \\ \frac{I'_{0^0}(P_i)+I'(P_i)}{2}, \; if \; I'_{0^0}(P_i) < 0 \\ and \\ \mathrm{I'}_{90^0}(P_i) \geq 0 \\ \frac{I'_{0^0}(P_i)+I'_{90^0}(P_i)+I'(P_i)}{2}, \; if \; I'_{0^0}(P_i) < 0 \\ and \\ I'_{90^0}(P_i) < 0 \\ \frac{I'_{90^0}(P_i)+I'(P_i)}{2}, \; if \; \mathrm{I'}_{0^0}(P_i) \geq 0 \\ and \\ I'_{90^0}(P_i) < 0 \end{cases} \tag{5}$$

$$LCP(P_0) = \{f_p(TD_r.f_1(x)), f_p(TD_r.f_2(x))...f_p(TD_r.f_8(x))\} \tag{6}$$

where the threshold task f_p (.,.)is depicted as

$$f_p(TD_r.f_i(x)) = \begin{cases} 1 & TD_r.f_i(x) > T \\ 0 & TD_r.f_i(x) \leq T \end{cases} \tag{7}$$

Where value of threshold T is delineated as,

$$T = TZ_d + TN_d \tag{8}$$

Figure 7.

For every Rs image field, we obtain a spatial histogram. For each R0, R1, R3 ..... By combining the histograms, R_s we get all the feature from the picture. This can be seen in figure 9.

4.1. Algorithm

The malaria detection algorithm using Local Composition Pattern (LCP) is shown below:

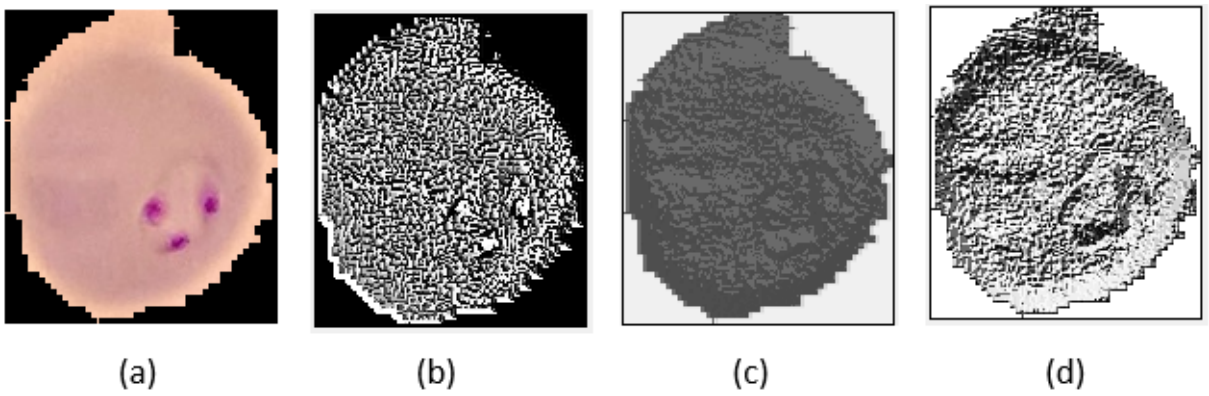

Figure 8. (a) Original image (b) LBP image (c) LDP image (d) LCP image

```
Input cell image I;
while each I do
    Divide I into 6 × 6 patches;
end
while each patch do
    while each pixel in patch of I do
        while alpha = 0^0,45^0,90^0,135^0,180^0,225^0,270^0,315^0
        do
            Apply Equation (1);
            if alpha=0^0,90^0 then
                Apply Equation (4);
                Apply Equation (5);
                Apply Equation (7);
                Apply Equation (8);
            end
        end
        Encode LCP applying Equation (6);
        Histogram concatenation of pixels in each patch;
    end
end
Histogram concatenation for different patches;
Return LCP;
```

5. Experiment and Result

With this criterion, our procedure gives a strong identification score. One is to adjust the values of parameters found in the SVM classifier. The sum of the termination requirements tolerance parameter $'eps'$ is set to 1.99 and $'c'$ (Cost parameter for C-SVC style classification) is set to 2.0, the gamma value is set to 0.0001, the $'nu'$ value is set to 0.0001 and the loss value is set to 0.001. Dividing the picture into various regions is another criterion. The provided image is divided into regions of 2×2,4×4,$6 \times 6$and measures the results and analyzes what gives the better results. After adjusting the parameter, it has been seen that LBP, LDP, LCP gives 60.7%, 57.2%, 63.25% respectively. Table 1. represents the compatibility of results with LBP, LDP and LCP.

Table 2 displays the different performance of area recognition. When the $'S'$ region is split into the 2×2 region recognition rate, it is 55.35%, where the vector distance of the function is 1024. But to improve the field, it provides much better precision. So we're dividing the areas

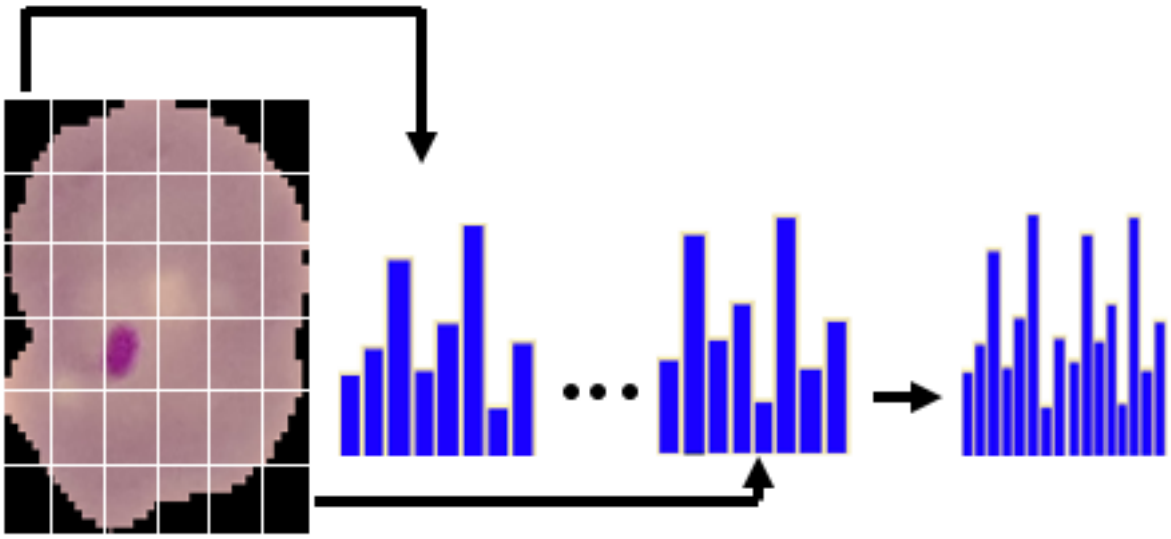

Figure 9. Concatenation of histogram of all the regions of an image

Table 1. Identification performance comparison

	Malaria detection (%)
LBP	60.7
LDP	57.2
LCP	63.25

Table 2. Identification performance of LCP in different region

	Malaria detection (%)	Vector length of LCP feature
s=2 × 2	55.35	1024
s=4 × 4	59.85	4096
s=6 × 6	63.25	9216

into 4×4. Where we can imagine a precision of 59.85%. In this instance, the vector distance of the LCP function is 4096, which is larger than the first one. Finally, we break the images into the 6×6 areas. We can see that our suggested descriptor gives a 63.25% recognition rate, where the vector length of the LCP function is 9216. From the '2' table we can make a conclusion that g=6×6 gives the highest precision.

In our algorithm, we have applied two distinct thresholds. To extract local characteristics, a fixed threshold is usually applied, but a high value threshold will pull out strong edges that can extract better features. We found a 62.9% identification rate when the threshold (T=0) for malaria infected cell image was found. But we can see that the recognition rate has risen to 63.25% since introducing our threshold. Where it is proven that the higher threshold is better in terms of performances which is listed in the table3.

6. Conclusion

The descriptor of a new local image feature descriptor, ′ Local Composition Pattern′, which is robust in detecting malaria, is described in the experimental work. We have applied a different

Table 3. Identification performance comparison for different threshold

	Malaria detection (%)
LCP (T=0)	62.9
LCP (T=SZ_d+SN_d)	63.25

mask to develop edge detection to get better characteristics accordingly. A fixed threshold where the given value is lower was added by other local feature descriptors, in some cases detecting weak edges is repeated edges. To establish this, we apply a smart and distinct threshold determined with the image's directional derivative of components that makes our work innovative. The experimental and result section specifically assesses that our approach provides a better recognition rate than the other descriptors.

References

[1] W. H. Organization, *World malaria report 2015*. World Health Organization, 2016.
[2] M. T. Makler, C. J. Palmer, and A. L. Ager, "A review of practical techniques for the diagnosis of malaria," *Annals of tropical medicine and parasitology*, vol. 92, no. 4, pp. 419–434, 1998.
[3] S. Foster and M. Phillips, "Economics and its contribution to the fight against malaria." *Annals of Tropical Medicine and Parasitology*, vol. 92, no. 4, pp. 391–398, 1998.
[4] P. B. Bloland, W. H. Organization *et al.*, "Drug resistance in malaria," Geneva: World Health Organization, Tech. Rep., 2001.
[5] M. Pammenter, "Techniques for the diagnosis of malaria." *South African medical journal= Suid-Afrikaanse tydskrif vir geneeskunde*, vol. 74, no. 2, pp. 55–57, 1988.
[6] C. Wongsrichanalai, M. J. Barcus, S. Muth, A. Sutamihardja, and W. H. Wernsdorfer, "A review of malaria diagnostic tools: microscopy and rapid diagnostic test (rdt)," *The American journal of tropical medicine and hygiene*, vol. 77, no. 6_Suppl, pp. 119–127, 2007.
[7] V. Batwala, P. Magnussen, and F. Nuwaha, "Comparative feasibility of implementing rapid diagnostic test and microscopy for parasitological diagnosis of malaria in uganda," *Malaria journal*, vol. 10, no. 1, p. 373, 2011.
[8] G. Cook, "Malaria: Obstacles and opportunities sc oaks, jr, vs mitchell, gw pearson & ccj carpenter (editors). washington, dc: National academy press, 1991. xv+ 309 pp. price£ 34.50. isbn 0-309-04527-4.[marketed and distributed in the uk by john wiley & sons, ltd, chichester]," 1992.
[9] N. E. Ross, C. J. Pritchard, D. M. Rubin, and A. G. Duse, "Automated image processing method for the diagnosis and classification of malaria on thin blood smears," *Medical and Biological Engineering and Computing*, vol. 44, no. 5, pp. 427–436, 2006.
[10] V. V. Makkapati and R. M. Rao, "Segmentation of malaria parasites in peripheral blood smear images," in *2009 IEEE International Conference on Acoustics, Speech and Signal Processing*. IEEE, 2009, pp. 1361–1364.
[11] F. B. Tek, A. G. Dempster, and I. Kale, "Parasite detection and identification for automated thin blood film malaria diagnosis," *Computer vision and image understanding*, vol. 114, no. 1, pp. 21–32, 2010.
[12] K. M.-a. Rao, A. Dempster, B. Jarra, and S. Khan, "Automatic scanning of malaria infected blood slide images using mathematical morphology," 2002.
[13] F. B. Tek, A. G. Dempster, and I. Kale, "Computer vision for microscopy diagnosis of malaria," *Malaria journal*, vol. 8, no. 1, p. 153, 2009.
[14] S. W. Sio, W. Sun, S. Kumar, W. Z. Bin, S. S. Tan, S. H. Ong, H. Kikuchi, Y. Oshima, and K. S. Tan, "Malariacount: an image analysis-based program for the accurate determination of parasitemia," *Journal of microbiological methods*, vol. 68, no. 1, pp. 11–18, 2007.
[15] L. Mirmohamadsadeghi and A. Drygajlo, "Palm vein recognition with local binary patterns and local derivative patterns," in *2011 International Joint Conference on Biometrics (IJCB)*. IEEE, 2011, pp. 1–6.
[16] B. A. Rosdi, C. W. Shing, and S. A. Suandi, "Finger vein recognition using local line binary pattern," *Sensors*, vol. 11, no. 12, pp. 11 357–11 371, 2011.
[17] U. Raju, A. S. Kumar, B. Mahesh, and B. E. Reddy, "Texture classification with high order local pattern descriptor: local derivative pattern," *Global Journal of Computer Science and Technology*, 2010.

[18] C. Shan, S. Gong, and P. W. McOwan, "Robust facial expression recognition using local binary patterns," in *IEEE International Conference on Image Processing 2005*, vol. 2. IEEE, 2005, pp. II–370.
[19] Z. Guo, L. Zhang, and D. Zhang, "A completed modeling of local binary pattern operator for texture classification," *IEEE Transactions on Image Processing*, vol. 19, no. 6, pp. 1657–1663, 2010.
[20] T. Ahonen, A. Hadid, and M. Pietikainen, "Face description with local binary patterns: Application to face recognition," *IEEE Transactions on Pattern Analysis & Machine Intelligence*, no. 12, pp. 2037–2041, 2006.
[21] J. E. Arco, J. M. Górriz, J. Ramírez, I. Álvarez, and C. G. Puntonet, "Digital image analysis for automatic enumeration of malaria parasites using morphological operations," *Expert Systems with Applications*, vol. 42, no. 6, pp. 3041–3047, 2015.
[22] D. Anggraini, A. S. Nugroho, C. Pratama, I. E. Rozi, A. A. Iskandar, and R. N. Hartono, "Automated status identification of microscopic images obtained from malaria thin blood smears," in *Proceedings of the 2011 International Conference on Electrical Engineering and Informatics*. IEEE, 2011, pp. 1–6.
[23] B. Zhang, Y. Gao, S. Zhao, and J. Liu, "Local derivative pattern versus local binary pattern: face recognition with high-order local pattern descriptor," *IEEE transactions on image processing*, vol. 19, no. 2, pp. 533–544, 2010.